Influence of Supplementary Oxide Layer on Solar Cell Performance

Mihai Oproescu
Faculty of Electronics, Communication and Computers, National University of Science and Technology POLITEHNICA Bucharest, Pitesti University Centre, Romania
mihai.oproescu@upb.ro (corresponding author)

Adriana-Gabriela Schiopu
Faculty of Mechanics and Technology, National University of Science and Technology POLITEHNICA Bucharest, Pitesti University Centre, Romania
gabriela.schiopu@upb.ro (corresponding author)

Valentin Marian Calinescu
Doctoral School Materials Science and Engineering, National University of Science and Technology POLITEHNICA Bucharest, Romania
valentin.calinescu@upit.ro

Vasile-Gabriel Iana
Faculty of Electronics, Communication and Computers, National University of Science and Technology POLITEHNICA Bucharest, Pitesti University Centre, Romania
vasile_gabriel.iana@upb.ro

Nicu Bizon
Faculty of Electronics, Communication and Computers, National University of Science and Technology POLITEHNICA Bucharest, Pitesti University Centre, Romania
nicu.bizon@upit.ro

Mohammed Sallah
Applied Mathematical Physics Research Group, Physics Department, Faculty of Science, Mansoura University, Egypt | Department of Physics, College of Sciences, University of Bisha, Saudi Arabia
msallahd@mans.edu.eg

Received: 8 January 2024 | Revised: 25 January 2024 | Accepted: 29 January 2024

 DOI: https://doi.org/10.48084/etasr.6879

ABSTRACT

The increasing use of solar energy for electricity production has led to a directly proportional growth in the production of solar cells. Photovoltaic (PV) performance of silicon solar cells can be improved by using more efficient technologies, optimizing processes, and changing behavior in order to reduce operational costs and greenhouse gas emissions. In order to propose solutions for commercial solar cell production with better performance, this article presents an experimental assessment on Supplementary Oxide Layers (SOLs) that are deposited on the surface of a solar cell absorber layer. SOLs are typically used to improve the performance of solar cells by passivating surface defects, reducing recombination losses, and improving the electrical contact between the absorber layer and the metal electrodes. The obtained solar cells are tested under natural sunlight conditions, following a variable dynamic electronic charge profile. The experimental results along with the corresponding I-V and P-V curves, are assessed according to the process parameters, the lighting parameters, and the dynamic load scenario. SOLs have been shown to improve the Power Conversion Efficiency (PCE) of solar cells considerably. The proposed method for increasing the energy efficiency of solar cells can be applied to any type of commercial solar cell and it is easy to implement at the industrial or research level by controlling process parameters. The integration of

the whole process, i.e. development of precursor solutions, deposition of thin films, and testing of electrical properties is another contribution of the current study, along with its interdisciplinary character, which involves materials science, electronics, and software programming.

Keywords-solar cells; energy efficiency; spin-coating deposition; metal-oxide film; software acquisition; characterization

I. INTRODUCTION

Starting with the first research in the field of capturing solar energy carried out by Antoine-César Becquerel around 1839, continuing with the development of the first physical model of the Solar Cell (SC) by Charles Fritts in 1883 and up to the present day, the improvement of operating and exploitation conditions, as well as the improvement of their energy efficiency were milestones in scientific research. Even if in 2021, charcoal remained the main fuel for electricity generation (its share being 36%) [1], in the context where worldwide energy production electricity in 2021 increased by 6.2%, a dynamic similar to that observed in 2010 as a result of the financial crisis, wind energy and solar energy reached a share of 10.2% of the total energy generated. It was the first time that wind and solar power have provided more than 10% of global electricity. The economic context, the conditions inflicted by the environmental protection, imposed photovoltaic (PV) energy as a viable source of renewable energy. As it can be seen from the dynamics of solar energy production [1], over 13% of the renewable energy is now produced with the help of SCs. The performance of SCs is influenced by several factors, such as:

- Climate. SCs are exposed to the environment for their entire life-time. Various factors affect the efficiency of the photoelectric conversion of an SC, including light, wind, and temperature [2]. In addition, some of these factors may damage the structure and functions of SC .
- Specific technological parameters, such as manufacturing technology and the types of basic materials used in SCs.
- Parameters of the output electronic converter: the type of electrical load and its dynamics, the type and number of power converters used in the output electronic circuit, the use of control algorithms for obtaining maximum energy - MPPT (Maximum Power Point Tracking).
- Energy efficiency refers to how energy is transformed, stored and utilized, as well as how products and technologies can be designed to reduce energy consumption [3, 4]. This can be applied to products, systems, and technologies.

A. Polycrystalline Solar Cells

Until now three generations of SCs have been reported. Crystalline silicon cells are the oldest and most developed solar panels. Unlike these, thin film cells are more flexible and 350 times thinner, aimed at industrial application for power energetics capacities. The type of semiconductor materials that are responsible for the photovoltaic (PV) effect represents the essential factor that distinguishes them. In thin film SCs, the semiconductor layer is placed between transparent conducting layers [5, 6]. Even though silicon is sometimes used to produce them, it is not the same as solid silicon wafer types, it is a non-crystalline type of silicon [7]. Typically, thin film SCs are manufactured by successively depositing thin films, with thicknesses between 1 and 10 μm, in a vacuum, on different substrates (such as polymer, glass, metal, and others) using etching technology to produce integrated modules over large areas. Multi-junction cells are produced based on high technology from two or more junctions layered on top of each other. Commercial viability is based on slowly depositing layers in systems, such as concentrated PV or space applications.

Silicon with different structural morphologies is usually employed for SCs. The production technology based on Si-wafers covered around 95% of the total production in 2020. PV technology production is significant because all manufacturing methods are conducted at low temperatures and on thin Si wafers with about 100 μm thickness. The use of silicon in SCs has been reduced significantly to about 3 g/Wp due to increased efficiencies and thinner wafers [5, 7]. The part of mono-crystalline technology is now about 84% of total Si solar cell production. Also, because it is mainly extracted from sand or quartz, it is 100% recyclable. Table I summarizes the characteristics of the best-reported polycrystalline commercial SCs. These commercial SCs have in common the type of applied Anti-Reflection Coating (ARC), namely Si_3N_4, as well as the front electrode, Ag and back electrode, Al. The differences are efficiency and the output power.

TABLE I. COMMERCIAL SOLAR CELLS CHARACTERISTICS

Type of silicon solar cell	Efficiency (%)	Output max. power (W)	ARC	Back electrode	Front electrode
Polycrystalline	17.8 ~ 18.8	4.33 ~ 4.58	Si_3N_4	Al	Ag
Polycrystalline	19.3 ~ 20.6	4.742 ~ 5.037	Si_3N_4	Al	Ag
Polycrystalline	18.1 ~ 18.9	4.4 ~ 4.57	Si_3N_4	Al	Ag
Polycrystalline	17 ~ 18.8	4.14 ~ 4.53	Si_3N_4	Al	Ag
Polycrystalline	19 ~ 19.6	4.668 ~ 4.816	Si_3N_4	Al	Ag
Polycrystalline	18 ~ 19.1	4.43 ~ 4.69	Si_3N_4	Al	Ag
Polycrystalline	17.8 ~ 18.9	4.33 ~ 4.6	Si_3N_4	Al	Ag, Al
Polycrystalline	18.40	4.478	Si_3N_4	Al	Ag
Polycrystalline	17.8 ~ 18.9	4.33 ~ 4.6	Si_3N_4	Al	Ag, Al
Polycrystalline	16.4 ~ 18.2	3.991 ~ 4.429	Si_3N_4	Al	Ag, Al

B. Metal Oxide Coatings

In recent studies, the use of some metal oxide films (ZnO, TiO_2, SiO_2, Al_2O_3, NiO, MgO) for the fabrication of SCs has been reported due to their superior electric and optical properties [8-15]. The metal oxide films present p or n-type conductivity and an energy gap around 3-7 eV. The deposition methods used are more and more varied: sol-gel, spin coating, chemical vapor deposition, physical vapor deposition, radio frequency-sputtering or printing. One of the best layer candidates is MgO, especially known for its high transmission value of about 91.48% in the visible range [11]. The current trends are to use MgO as an intermediate layer in perovskite, dye sensitized, or polymer SCs [12-14]. For perovskite SCs, a magnesium oxide layer was achieved in [15] via decomposition of magnesium acetate on mesoporous TiO_2. The obtained efficiency increased to 13.9%. Also, a MgO layer was successfully incorporated between SnO_2 and F-doped tin oxide to increase the PCE from 16.4% to 18.23% in [16]. Nanostructured MgO films, using spray pyrolysis on glass substrate show a good transmittance of 90% [17]. The optical band gap between 3.64 and 3.7 eV make these films usable for protective layers in SCs, a anti-reflective coating MgO of 86 nm thickness reduces reflectivity to 30% compared to a normal solar cell [18]. In [19], MgO nanostructured films were deposited on a glass substrate using Nd-YAg laser ablation of a methanol solution. The uniform obtained films of a p-MgO/n-Si solar cell structure had a good optical transparency and a low refractive index with increasing wavelength [19]. Enhancement in the photocurrent and the voltages was found in solid-state dye sensitized cells fabricated with MgO coatings on nanocrystalline SnO2, as anode and CuI as cathode [20].

II. MATERIALS AND METHODS

A. Choice of Oxide

Magnesium oxide was chosen as the precursor material due to its nontoxicity, physical stability, high transmission value in visible range, and the wide direct band gap of 7.8 eV. It is very stable at high temperatures in oxidizing atmospheres up to 2300 °C and reducing atmospheres at 1700 °C, respectively, while it crystallizes in the cubic rock-salt type (cell parameter 4.21 Å) [21]. The hygroscopic nature of MgO and its transition to $Mg(OH)_2$ are often mentioned in experimental research with the statement that MgO is generally stable.

B. Choice of Solvents

For the realization of MgO coatings, 3 solvents were chosen: ethanol (EtOH), ethanolamine (EA), and ethylene glycol (EG). MgO is not soluble in any of the chosen solvents and can be safely dispersed without dissolution. EtOH has lower polarity and evaporates the fastest. EtOH evaporates completely after 25-30 min. EA has a low vapor pressure at room temperature, and the rate of evaporation increases with increasing temperature. EG is a symmetrical molecule and it can be believed that it has a permanent dipole moment. However, its C-OH bonds rotate, which favors dipoles. It is also a dynamic molecule, which undergoes constant rotations and vibrations, and can form or receive hydrogen bonds thanks to its two OH groups. EG evaporates completely at 197.2 °C.

To obtain the precursor solutions, 2g MgO (Roth reagent, analytical grade) was dispersed in 100 ml of each solvent: Et-OH, EA, and EG, on ultrasonic bath, for 90 s, generating different solutions. The pH of the precursor solutions is in the basic range, having the following values: 11 corresponding to the dispersion of MgO in EtOH, 12.75 corresponding to the dispersion of MgO in EA, respectively, 10.33 for the dispersion of MgO in EG. No binder was used because it can lead to changes in the properties of the coatings.

C. Spin Coating Procedure

The spin coating method was chosen for developing coatings because it can be implemented in a wide variety of productions and technology sectors. Its primary advantage over the other methods is its ability to fast and easily produce very uniform and adherent coatings. Commercial polycrystalline silicon SC (poly-Si) pieces for experimental procedure with dimensions of 5.2×1.9 cm were cleaned in the ultrasonic bath in ethanol and deionized water for 180 s for each cleaning agent. The cleaning process aimed to remove impurities (e.g. grease, dust). At the first stage of the deposition, 100 µl of each precursor solution was added to a small rotation on the top of the polycrystalline silicon SC (dynamic spin coating). The rotation speed of the SCV-10 spin-coater was initially set to 25 rps, i.e. 1500 rpm. In the second stage, 4 drops of 50 µl, at intervals of 30 s, at 2000 rpm, were added. In the third stage, the covered commercial SC was heat treated between 850 °C and 1200 °C for 10 min on the hotplate MS-H280-Pro. The characteristic parameters of deposition are presented in Table II and the deposition process is schematically shown in Figure 1.

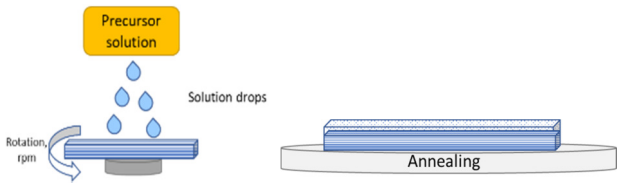

Fig. 1. Deposition process.

TABLE II. CHARACTERISTICS OF SPIN-COATING DEPOSITION OF MGO COATINGS

Solar cell code	Synthesis parameters	Total volume of precursor solution (µl)	Time process (min)
poly-Si/MgO/EtOH/0.3 poly-Si/MgO/EA/0.3 poly-Si/MgO/EG/0.3	1 drop of 100 µl at 1500 rpm, time 30 s 4 drops of 50 µl at 30 s range, 2000 rpm	300	3
poly-Si/MgO/EA/1.1	1 drop of 100 µl at 1500 rpm, time 30 s 10 drops of 100 µl at 30 s range, 2000 rpm	1100	6
poly-Si/MgO/EG/1	1 drop of 100 µl at 1500 rpm, time 30 s 9 drops of 100 µl at 30 s range, 2000 rpm	1000	6

D. Microscopic Characterization

The way of crystallization and formation of the SOL was observed by the optical microscopic method using the digital microscope Hayer Hy-2070. The results of the microscopic analysis are presented in Figure 2.

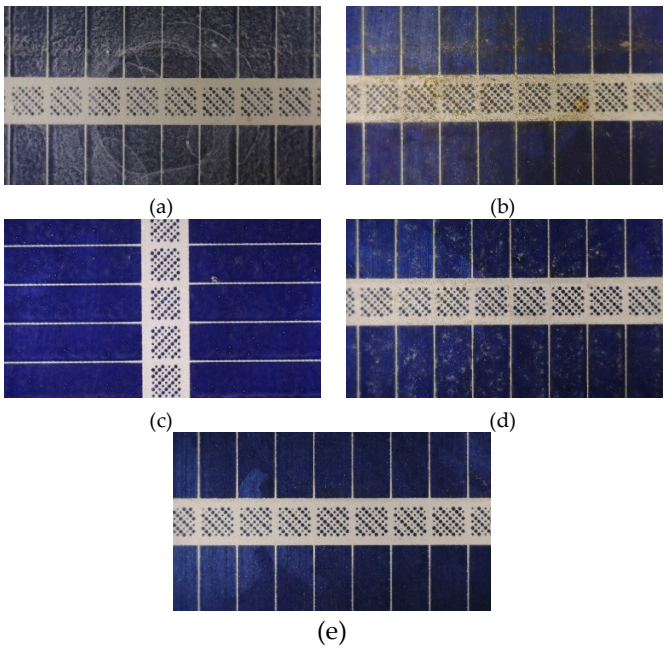

Fig. 2. Microscopic analysis of layers: (a) poly-Si/MgO/EtOH/0.3, (b) poly-Si/MgO/EA/0.3, (c) poly-Si/MgO/EG/0.3, (d) poly-Si/MgO/EA/1.1, (e) poly-Si/MgO/EG/1.

Microscopy analysis indicates the formation of some crystallization nuclei agglomerated towards the center of the cell corresponding to small amounts of precursor solutions. At the same time, it was noticed that when adding larger volumes (1 ml), the deposits WERE uniformly crystallized.

E. Optical characterization

The three dispersions OF MgO in EtOH, EA, and EG were subjected to UV-Visible spectroscopy by Ocean Optics HR2000+ in the range of 200-800 nm in order to get maximum absorbance, as can be seen in Figure 3.

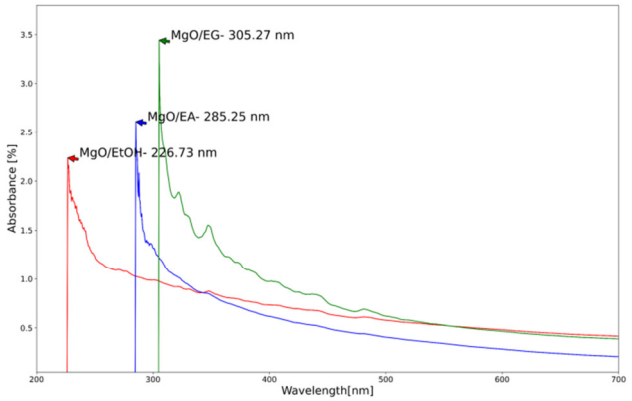

Fig. 3. UV-VIS spectra of MgO in EtOH, EA, EG.

MgO particles in EtOH exhibit a characteristic absorption peak in the ultraviolet (UV) region of the spectrum, typically around 226 nm. The UV-visible absorption spectrum of MgO particles in EA is similar to that in EtOH, with a characteristic absorption peak in the UV region of the spectrum, typically around 285 nm. This peak arises from the excitation of electrons from MgO's valence band to its conduction band. EA is a more polar molecule than EtOH, and this led to stronger interactions between the MgO particles and the EA molecules, which affect the absorption properties of the particles. As can be seen from the spectrum, the absorption peak around 285 nm is still quite pronounced, indicating strong UV absorption. The steep rise in absorption at shorter wavelengths suggests that MgO particles in EA absorb UV light efficiently. The UV-Vis absorption spectrum of MgO particles in EG is similar to that in EtOH and EA, with a characteristic absorption peak in the UV region of the spectrum, around 305 nm. EG is a more viscous solvent than EtOH and EA, and this may make it more difficult for the MgO particles to diffuse freely in the solvent. However, the absorption coefficient is slightly higher than that in EtOH and EA. The absorption properties of MgO nanoparticles in EG are of interest for SOL elaboration on poly-crystalline SCs.

III. SOLAR CELL TESTING SYSTEM

In accordance with the main objective of the experimental research, increasing the energy efficiency by obtaining SC covered with advanced SOL, a hardware & software system was designed and developed for the control of operating parameters and real-time monitoring of SC [22, 23]. Thus, the system of data acquisition and control of parameters was developed, in accordance with the software application for the fusion of data from the variation of ambient parameters (temperature, lighting) and functional electrical parameters of the SC (no-load voltage, load voltage, current short circuit).

A. Solar Cell Testing System

The proposed system for the control and acquisition of parameters that influence the operation of SCs is displayed in Figure 4. The testing system consists of:

- Solar cell block: In this block we find the SC type UFY002914 [22].
- Controlled electronic load block: It is implemented through a current source that fixes the current through the solar cell in the 0-30 mA range.
- Acquisition and control bloc.
- Stabilized, controlled power supply: This source provides the continuous voltages used by the other building blocks.

Each SC is connected to a controlled electronic load. All six electronic loads are synchronously controlled, using the same control parameters. For the experiments, 100 values were imposed for the load current through each solar cell, between 0 mA (open circuit) and 50 mA. The acquisition started 1 s after each value of the current was set. For each set value of the current, 50 values were considered for the solar cell voltage and 50 values for the current were drawn by the SC. The experiment was conducted as see in Figure 5.

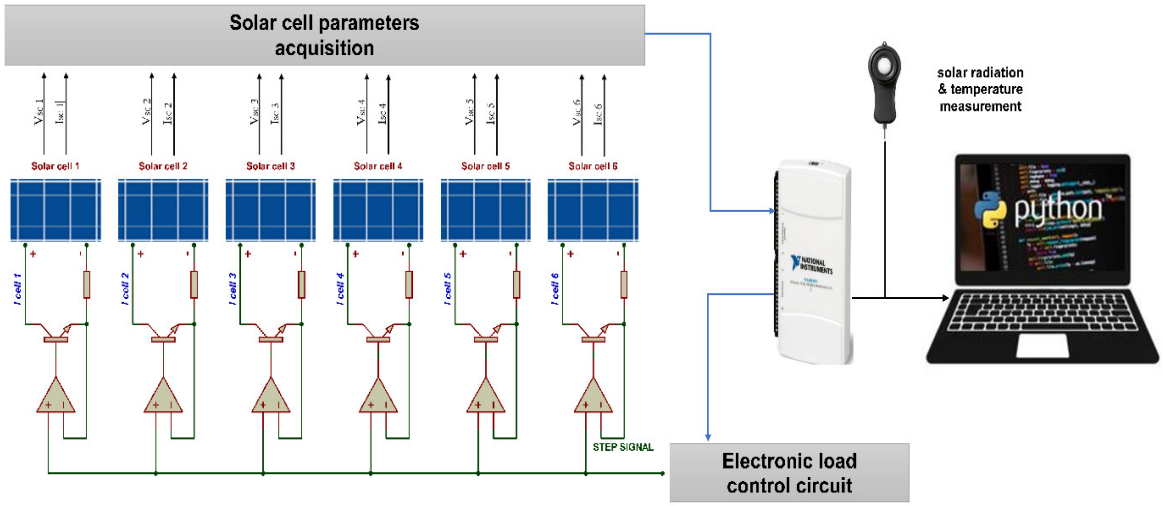

Fig. 4. Control system and acquisition of parameters from SCs using real atmospheric conditions.

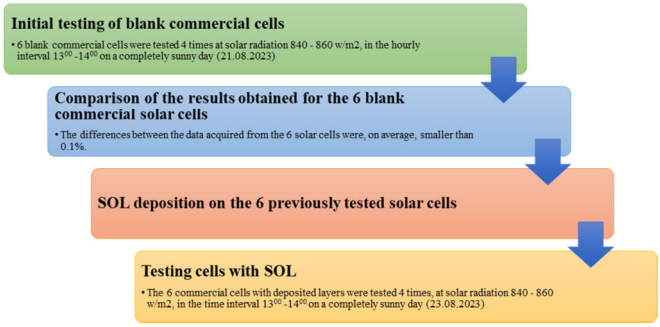

Fig. 5. The experimental process.

The entire management regarding the establishment of the parameters of the lighting level, the level of electronic load and the acquisition of SC parameters (V, I) in accordance with the set parameters, was carried out with the help of the acquisition and control board NI USB 6211 [22]. Its purchasing interface has, according to the manufacturer's data, the following input/output ports: 16 analog input channels (16 bits, 250 kS/s), 2 analog output channels (250 kS/s), and 8 digital input/output channels. In the case of the experiments carried out, the following of these were used: 2-analog inputs for the acquisition of the voltage of the solar cell and 1 analog output for controlling the electric output load. At the same time, the connection with the Python software application was made through the NI USB 6211. Pyhton software was implemented to generate comparative graphs between the parameters of 2, 3, or more SCs, and the loaded vectors already having the optimal structure.

IV. RESULTS AND DISCUSSION

A. Comparative Analysis of I-V, P-V Characteristics

Each SC was subjected to tests in order to establish the I-V and P-V capacities, one without additional layers deposited and one after the deposition of oxide layers. The conditions for the electric charge at the output have always been the same, with the current through the load ranging from 0 to the maximum value I_{sc}. In the first stage, testing of the 6 standard p-type commercial SCs (SC_com), without MgO coatings, was carried out (see Figure 6). No significant differences were found (variation of less than 0.2%) between the purchased parameters. Subsequently, the 6 p-type SCs covered with MgO films, from different solutions and different process parameters, were tested at the same conditions, to obtain information about the energy efficiency evolution of the coatings. In order to have the most accurate picture of the acquired values, each test was repeated 5 times, under approximately similar conditions, obtaining 5 value vectors for each performed test. Table III presents the correlation between the tests performed and the characteristics of the tested cells.

TABLE III. CORRELATION BETWEEN THE TESTS PERFORMED AND THE CHARACTERISTICS OF THE TESTED CELLS

Test cod	Solar cell sample
TEST 1	Average value for 6 SC_com – SC_com
TEST 2	Poly-Si/MgO/EG/0.3
TEST 3	Poly-Si/MgO/EA/1.1
TEST 4	Poly-Si/MgO/EA/0.3
TEST 5	Poly-Si/MgO/EG/0.5
TEST 6	Poly-Si/MgO/EtOH/0.3
TEST 7	Poly-Si/MgO/EG/1.0

The next stage was to conduct comparative analysis using the results of two or three tests as input values. For accuracy, this analysis was carried out taking into account the synthesis parameters of MgO coatings. The results of the testing led to the realization of a database, with 12000 values for each cell tested, including the values of the output voltage V, the value of the current by load I, and the value of the output power P. Analyzing the results (Figure 7) for SC_com versus the poly-Si/MgO/EtOH/0.3 cell, it can be revealed that the current intensity value through the SC and the output power measured, are higher for the SC_com. These characterizations conclude that the EtOH solvent does not advantage the deposition of a MgO coating considering as goal the increasing of SC energy efficiency. The comparative analysis of the efficiency of MgO coatings obtained with EA and EG, at different solution volumes, is shown in Figure 7.

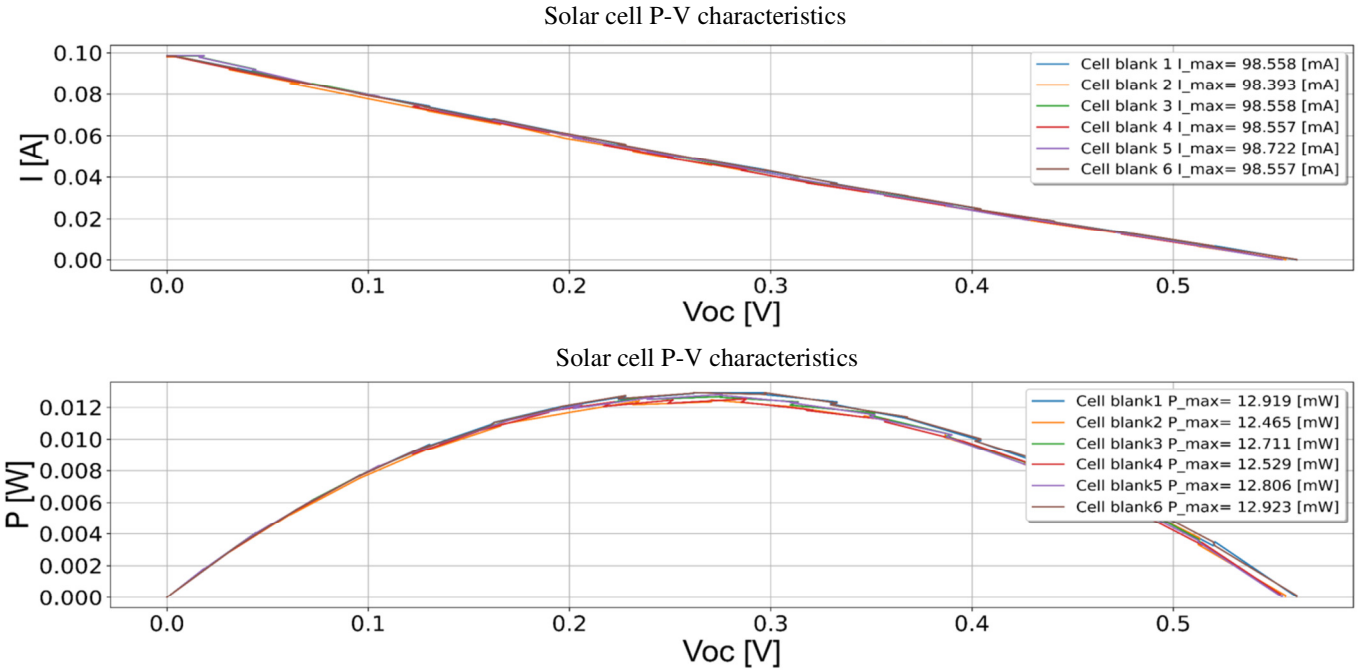

Fig. 6. Comparative analysis of I-V and P-V for six commercial cells before the deposition of additional layers.

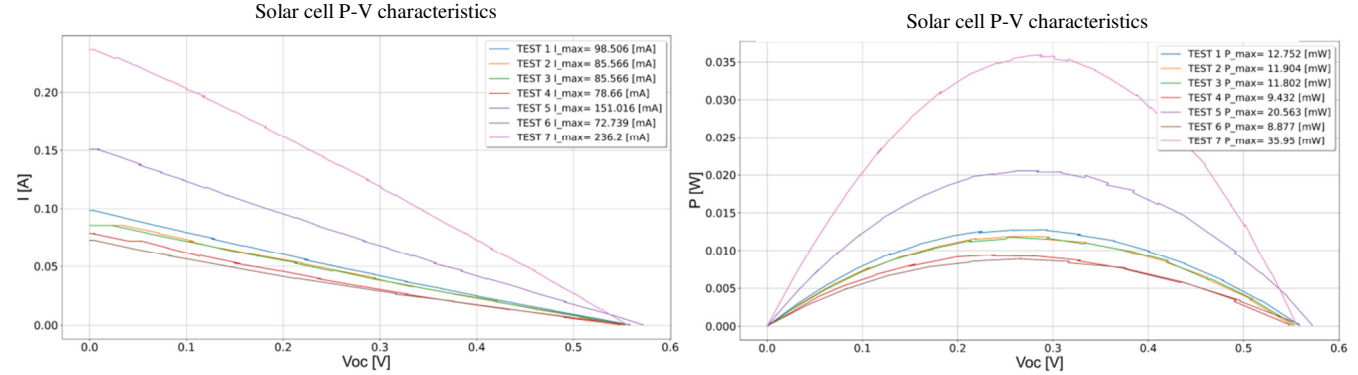

Fig. 7. Comparative analysis I-V, P-V between six commercial cells (after the deposition of additional layers) and the average value before the deposition of additional layers, TEST 1 - average value for 6 commercial SCs (blue), TEST 2 - Poly-Si/MgO/EG/0.3 (green), TEST 3 - Poly-Si/MgO/EA/1.1 (orange), TEST 4 - Poly-Si/MgO/EA/0.3 (red), TEST 5 - Poly-Si/MgO/EG/0.5 (magenta), TEST 6 - Poly-Si/MgO/EtOH/0.3 (brown), TEST 7 - Poly-Si/MgO/EG/1.0 (pink).

Comparing the results of testing the SC_com versus the poly-Si/MgO/EA/0.3 cell, it can be said that the current intensity value through the cell and the measured output power, are also higher in the case of SC_com. The average value (the average of the values recorded in the 5 acquisitions of the same test) of the maximum power determined is about 37% (3.53 W/m^2) higher in the case of SC_com versus the poly-Si/MgO/EA/0.3 cell. Also, the value of the open voltage (without load) for the poly-Si/MgO/EA/0.3 cell is smaller than that of the SC_com cell. These characterizations conclude that EA does not significantly favor increasing the energy efficiency of the MgO coatings on SCs, for the synthesis conditions, therefore the experimental protocol has been modified. To verify its influence on the electrical properties, volume solution was increased.

The intensity of the current through the SC and the output power measured for SC_com versus poly-Si/MgO/EA/1.1 cell, are smaller in the case of poly-Si/MgO/EA/1.1 cell with an average decrease value of 14.22 mA. The average power value of poly-Si/MgO/EA/1.1 cell is smaller than the power value of the SC_com by 9.49%. Even if the average value of the electrical power offered by poly-Si/MgO/EA/1.1 is still lower than in the case of SC_com, a substantial increase in the power of poly-Si/MgO/EA/1.1 can be observed, compared to the SC covered with the same solvent, but with a smaller volume (poly-Si/MgO/EA/0.3), with 2,399 W/m^2 (25%). The results confirm that the EA solvent favors the formation of MgO coatings that can offer increasing energy efficiency at increased volumes (greater than 1 ml).

The same comparative analyzes were performed for the EG solvent, for different solution volumes. The maximum value of the current intensity for SC_com cell versus poly-Si/MgO/EG/0.3 cell was about the same, but higher for the SC_com. In the case of the poly-Si/MgO/EG/0.3 cell, an approximately constant value of the maximum current was acquired for all measurements. The average power value of

poly-Si/MgO/EG/0.3 cell is less than the power of the SC_com, but the differences are not significant, with percentage differences around 4% (4,98 W/m^2).

Following these characterizations, it is observed that the EG solvent favors the increase of the current intensity value, compared to the other two solvents. This result agrees with the fact that the absorption coefficient of MgO in EG is slightly higher than that in EtOH and EA and can lead to the formation of more absorbent layers in the UV region. Respecting the previous reasoning of research, the experimental protocol was modified in terms of the volume of the dropped solution.

The output power measured for the SC_com was lower than that of the poly-Si/MgO/EG/0.5, the average difference being 49.5 mA. The power of the poly-Si/MgO/EG/0.5 cell, is greater than the power of the SC_com by an average of 59.59%. After obtaining these results, the increase of the volume of solvent deposited on the SC_com (1 ml) was continued. The output power measured for poly-Si/MgO/EG/1 cell was higher than that of SC_com with an average difference of 135.6 mA (182%). Compared to the same solvent, but for a smaller quantity (0.5 ml - poly-Si/MgO/EG/0.5), poly-Si/MgO/EG/1 offers an average increase of 36.36 W/m^2.

When using the same increased amount (1 ml) of precursor solution, but changing the type of solvent (EA vs. EG) the following results were achieved. The average value of the power obtained in the case of poly-Si/MgO/EG/1 is higher than in the case of the test poly-Si/MgO/EA/1.1 by 24.7 W/m^2. It is obvious that the use of the EG solvent leads to obtaining an MgO coating characterized by increased electric power. In average value, the resulting power for poly-Si/MgO/EG/1 cell is 206.8% higher than for poly-Si/MgO/EA/1.1 cell.

B. Comparative Energy Efficiency Analysis for the Tested Cells

Energy efficiency refers to how much electricity can be generated by an SC in a given time frame. The energy efficiency of SCs may vary depending on the type and quality of the SCs used, but also on other external factors. The efficiency of commercial SCs generally varies between 10 and 23%, depending on their type and quality. The efficiency of polycrystalline SCs is measured by the ratio between the electrical power generated by the cell and the sunlight energy absorbed by it. In general, polycrystalline SCs have a lower efficiency than monocrystalline SC, around 15-16%. Also, the energy efficiency of SCs can be improved by using special materials or by applying advanced technologies. High-performance SCs have been obtained under laboratory conditions with efficiencies of more than 26% [9]. In this paper, for the calculation of the energy efficiency of the solar cell we used the following relationship:

$$\eta_{solar\ cell} = \frac{P_{max-solar\ cell}}{Surface \times Incident\ radiation\ flux} \times 100 \quad (1)$$

where *Surface* = 0,000988 m^2, $P_{max\text{-}solar\ cell}$ [W] are the values acquired from the tested SCs, and incident radiation flux was measured with Voltcraft PL-110SM digital pyranometer, considering 3 scenarios: under Standard Test Conditions (STC-Irradiance 1000 W/m^2, Cell Temperature 25 °C, AM1.5), under Nominal Module Operating Temprature (NMOT - Irradiance 800 W/m^2, Ambient Temperature 20 °C, AM1.5, Wind Speed 1 m/s), and under REAL operating conditions (lrradiance 840 W/m^2, Ambient Temperature 28 °C, AM1.5). The comparative analysis of the energy efficiency of SCs coated with MgO layers obtained from different precursor solutions is portrayed in Figures 8 and 9.

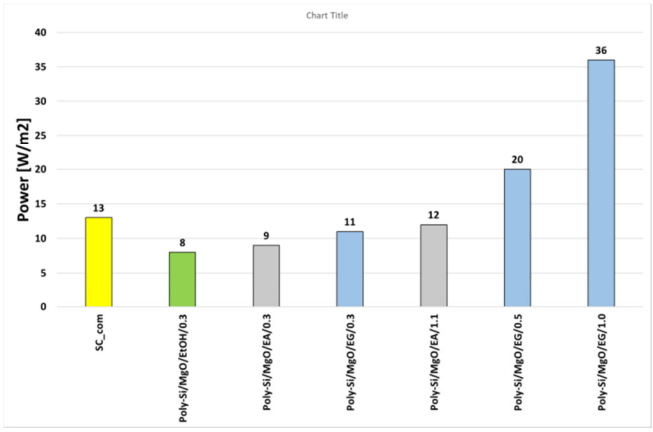

Fig. 8. Power energy of MgO coatings, obtained from different solvents [W/m^2].

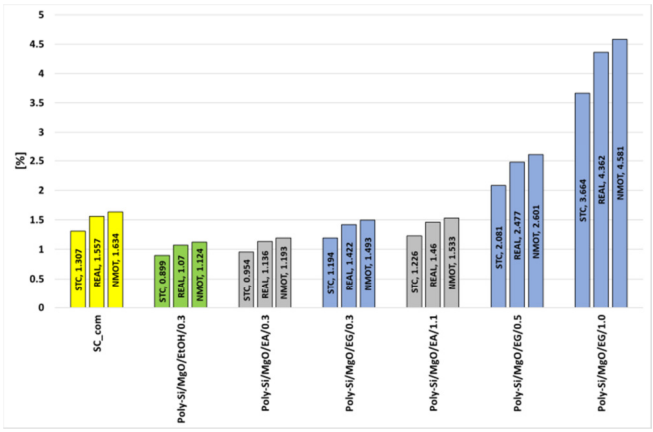

Fig. 9. Energy efficiency of MgO coatings, obtained from different solvents and for different operating conditions (yellow – blank SC, green – EtOH, gray – EA, blue – EG) in [%].

As in the case of the power flown by the tested SCs and in the case of energy efficiency (there is a direct dependence between these parameters), the best results sdfd obtained for volumes of 1 ml solvent (for EA and EG), (see Figures 8, 9). Using the EtOH, it is observed that the efficiency of MgO deposited SCs was significantly lowered compared to the uncoated SCs. Making a comparison between polycrystalline SCs coated with additional coatings with the uncoated cells (Figure 10), where the uncovered cell represents the zero axis, we note that only poly-Si/MgO/EG/0.5 and poly-Si/MgO/EG/1 cells offer improved energy efficiency. If we utilize the same conditions as in the case of poly-Si/MgO/EG/1 cell to cover a commercial solar panel Sharp ND-RB270 [24, 25] of 164.9 W/m^2 and 16.5% efficiency, the new output power, on the STC favorable conditions (no shading, temperatures in the nominal operating range) increases up to 262.4 W/m^2 and 26.2%.

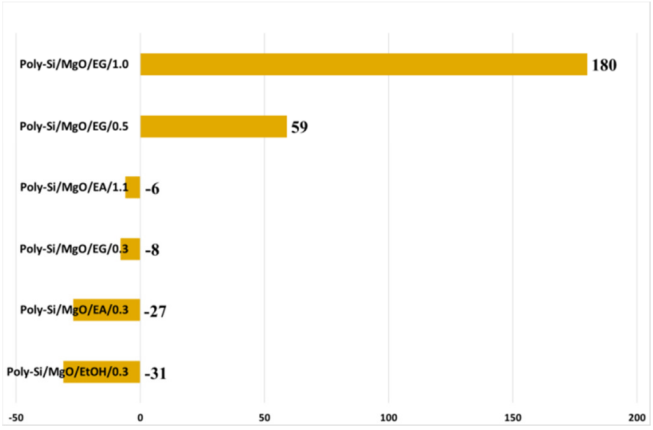

Fig. 10. Increase / decrease of energy efficiency percentage compared to the average efficiency value of commercial blank cells.

V. CONCLUSIONS

The novelty of this paper is supported by the following aspects: (a) The presented method for increasing the energy efficiency of Solar Cells (SCs) is applicable for any type of commercial silicon SCs. (b) For certain process parameters (type of solvent used and volume of solution applied), an electric power value almost twice that of the same cell without additional layer was obtained. (c) The implementation of the deposition process at an industrial level has low costs.

The main contributions of the paper are represented by the development of additional oxide layers deposited on commercial SCs, starting from MgO, dispersed in different solvents, which lead to the increase of electrical power, compared to the same SCs without additional layers and the realization of a complex system for testing SCs.

- MgO coatings have been successfully obtained on commercial polycrystalline SCs by spin-coating deposition starting from the dispersion of MgO into different solvents. Testing of electrical properties of the coated SCs in real conditions indicates that additional MgO coatings can increase energy efficiency. The carried out comparative analysis of the tests shows the importance of the deposition process of additional layers to improve the electrical performance of SCs. The experimental characterization was performed for the over 12000 recorded values of current intensity and output power, specific to each tested cell.
- Under the conditions of using ethanolamine solvent, a slight improvement of power was observed only when the volume of the deposited solution reached 1 ml. For smaller solution volumes, the obtained coating did not provide a substantial conversion of light into electricity.
- The current intensity through the solar cell and the output power measured are higher in the case of poy-Si.MgO/EG/1, corresponding to MgO coating by spun of 1 ml ethylene glycol precursor solution. The power of these is greater than the power of the commercial cell by 180%.
- Regarding the spin-coating method of synthesizing MgO coatings, it is recommended to use volumes larger than 1 ml to achieve a uniform film at a high rotational speed (2000 rpm), with 30 s time interval between droplets, and total process time of 6 min.

Future research will focus on testing the influence of adding additional layers on commercial polycrystalline cells, testing the energy efficiency of the layers added by the spraying method combined with spin coating, the use of other types of metal oxides (e.g. ZnO), and defining the life span of a cell coated with MgO films. The use of magnesium oxide nanoparticles (through solar energy through SPVD - Solar Physical Vapor Deposition) in different volumes of solvent and at different parameters of the deposition process is also a concern for further studies.

REFERENCES

[1] "Renewable electricity generation," *Our World in Data*. https://ourworldindata.org/grapher/modern-renewable-energy-consumption.

[2] M. Jomaa, M. Abbes, F. Tadeo, and A. Mami, "Greenhouse Modeling, Validation and Climate Control based on Fuzzy Logic," *Engineering, Technology & Applied Science Research*, vol. 9, no. 4, pp. 4405–4410, Aug. 2019, https://doi.org/10.48084/etasr.2871.

[3] A. Alanazi, "Optimization of Concentrated Solar Power Systems with Thermal Storage for Enhanced Efficiency and Cost-Effectiveness in Thermal Power Plants," *Engineering, Technology & Applied Science Research*, vol. 13, no. 6, pp. 12115–12129, Dec. 2023, https://doi.org/10.48084/etasr.6381.

[4] F. Mavromatakis, Y. Franghiadakis, and F. Vignola, "Modeling Photovoltaic Power," *Engineering, Technology & Applied Science Research*, vol. 6, no. 5, pp. 1115–1118, Oct. 2016, https://doi.org/10.48084/etasr.612.

[5] S. Ho, "A Review of Metal Oxide Thin Films in Solar Cell Applications," *International Journal of Thin Film Science and Technology*, vol. 11, no. 1, pp. 37–45, Jan. 2022, https://doi.org/10.18576ijtfst/110105.

[6] M. Jlassi, I. Sta, M. Hajji, and H. Ezzaouia, "NiO thin films synthesized by sol-gel: Potentiality for the realization of antireflection layer for silicon based solar cell applications," *Surfaces and Interfaces*, vol. 6, pp. 218–222, Mar. 2017, https://doi.org/10.1016/j.surfin.2016.10.006.

[7] Y. Lee, C. Park, N. Balaji, Y.-J. Lee, and V. A. Dao, "High-efficiency Silicon Solar Cells: A Review," *Israel Journal of Chemistry*, vol. 55, no. 10, pp. 1050–1063, 2015, https://doi.org/10.1002/ijch.201400210.

[8] I. Zeghib and A. Chaker, "Efficiency of a Solar Hydronic Space Heating System under the Algerian Climate," *Engineering, Technology & Applied Science Research*, vol. 6, no. 6, pp. 1274–1279, Dec. 2016, https://doi.org/10.48084/etasr.875.

[9] S. Kim, J. Park, P. D. Phong, C. Shin, S. M. Iftiquar, and J. Yi, "Improving the efficiency of rear emitter silicon solar cell using an optimized n-type silicon oxide front surface field layer," *Scientific Reports*, vol. 8, no. 1, Jul. 2018, Art. no. 10657, https://doi.org/10.1038/s41598-018-28823-x.

[10] A. M. Mouafki, F. Bouaicha, A. Hedibi, and A. Gueddim, "Porous Silicon Antireflective Coatings for Silicon Solar Cells," *Engineering, Technology & Applied Science Research*, vol. 12, no. 2, pp. 8354–8358, Apr. 2022, https://doi.org/10.48084/etasr.4803.

[11] B. R. Ali, "Synthesis And Characterization Of Nanoparticles Mgo Films On Silicon Substrates For Solar Cells Applications," *Journal of Multidisciplinary Engineering Science Studies*, vol. 2, no. 7, pp. 610–612, 2016.

[12] A. Kulkarni, A. K. Jena, H.-W. Chen, Y. Sanehira, M. Ikegami, and T. Miyasaka, "Revealing and reducing the possible recombination loss within TiO2 compact layer by incorporating MgO layer in perovskite solar cells," *Solar Energy*, vol. 136, pp. 379–384, Oct. 2016, https://doi.org/10.1016/j.solener.2016.07.019.

[13] S. Huang, B. Kang, L. Duan, and D. Zhang, "Highly efficient inverted polymer solar cells by using solution processed MgO/ZnO composite interfacial layers," *Journal of Colloid and Interface Science*, vol. 583, pp. 178–187, Feb. 2021, https://doi.org/10.1016/j.jcis.2020.09.047.

[14] J. Dagar, S. Castro-Hermosa, G. Lucarelli, F. Cacialli, and T. M. Brown, "Highly efficient perovskite solar cells for light harvesting under indoor illumination via solution processed SnO2/MgO composite electron transport layers," *Nano Energy*, vol. 49, pp. 290–299, Jul. 2018, https://doi.org/10.1016/j.nanoen.2018.04.027.

[15] X. Guo, H. Dong, W. Li, N. Li, and L. Wang, "Multifunctional MgO Layer in Perovskite Solar Cells," *ChemPhysChem*, vol. 16, no. 8, pp. 1727–1732, 2015, https://doi.org/10.1002/cphc.201500163.

[16] J. Ma *et al.*, "MgO Nanoparticle Modified Anode for Highly Efficient SnO2-Based Planar Perovskite Solar Cells," *Advanced Science*, vol. 4, no. 9, 2017, Art. no. 1700031, https://doi.org/10.1002/advs.201700031.

[17] O. Diachenko *et al.*, "Surface Morphology, Structural and Optical Properties of MgO Films Obtained by Spray Pyrolysis Technique," *Acta Physica Polonica A*, vol. 3, no. 130, pp. 805–810, 2016, https://doi.org/10.12693/APhysPolA.130.805.

[18] B. Dhamodharan and S. Periyasamy, "Analysis of Solar Cell with MGO Anti-Reflective Coating," *International Journal for Scientific Research & Development*, vol. 4, no. 4, pp. 415–417, Jan. 2016.

[19] J. You *et al.*, "Improved air stability of perovskite solar cells via solution-processed metal oxide transport layers," *Nature Nanotechnology*, vol. 11, no. 1, pp. 75–81, Jan. 2016, https://doi.org/10.1038/nnano.2015.230.

[20] S. Perera *et al.*, "The Effect of MgO on the Enhancement of the Efficiency in Solid-State Dye Sensitized Photocells Fabricated with SnO2 and CuI," *Bulletin of the Chemical Society of Japan*, vol. 76, no. 3, pp. 659–662, Mar. 2003, https://doi.org/10.1246/bcsj.76.659.

[21] T. Huma, N. Hakimi, M. Younis, T. Huma, Z. Ge, and J. Feng, "MgO Heterostructures: From Synthesis to Applications," *Nanomaterials*, vol. 12, no. 15, Aug. 2022, Art. no. 2668, https://doi.org/10.3390/nano12152668.

[22] V. Calinescu, M. Oproescu, G.-V. Iana, O. C. Novac, and M. C. Novac, "Efficiency of Nanostructured Layers Deposited on Solar Cells - hardware system proposal," in *14th International Conference on Electronics, Computers and Artificial Intelligence*, Ploiesti, Romania, Jul. 2022, pp. 1–6, https://doi.org/10.1109/ECAI54874.2022.9847309.

[23] A. Elgharbi, D. Mezghani, A. Mami, and A. Gharbi, "Intelligent Control of a Photovoltaic Pumping System," *Engineering, Technology and Applied Science Research*, vol. Vol.9, pp. 4689–4694, Oct. 2019, https://doi.org/10.48084/etasr.2982.

[24] "Sharp ND-RB270." https://www.europe-solarstore.com/sharp-nd-rb270.html?gad_source=1&gclid=CjwKCAiAyp-sBhBSEiwAWWzTnqRIPK-ur7_DQeIKmS18s-d_D7ZgrJ5yw7we5dk_b9TCQSPnrfOXnBoCN0EQAvD_BwE.

[25] M. E. Bendib and A. Mekias, "Solar Panel and Wireless Power Transmission System as a Smart Grid for Electric Vehicles," *Engineering, Technology & Applied Science Research*, vol. 10, no. 3, pp. 5683–5688, Jun. 2020, https://doi.org/10.48084/etasr.3473.